

ANOMALOUS ROTATIONAL DAMPING IN
FERROMAGNETIC SHEETS

T. L. Gilbert and J. M. Kelly

Armour Research Foundation of
Illinois Institute of Technology
Chicago, Illinois

ABSTRACT

A previously unexplored method is presented for determining the anomalous damping in ferromagnetic sheets by measuring the torque on a thin ferromagnetic disk in a strong rotating field. The relation between the torque and the anomalous damping parameter is derived from a steady-state solution of the damped spin-wave equation,

$$d\mathbf{M}/dt = \gamma \mathbf{M} \times [\mathbf{H} - (\alpha/\gamma\mathbf{M}) d\mathbf{M}/dt],$$

and Maxwell's equations. This spin-wave equation follows rigorously from the Landau-Lifshitz equation if one sets

$$\alpha = (\lambda/\gamma\mathbf{M})(1 + \lambda^2/\gamma^2\mathbf{M}^2)^{-1} \leq 1/2$$

and replaces γ by $\gamma(1 + \lambda^2/\gamma^2\mathbf{M}^2)$. An explicit steady-state solution is calculated for an isotropic sheet and for an anisotropic sheet with an infinite exchange stiffness. Preliminary measurements on commercially rolled sheets of 4-79 Molybdenum Permalloy, 3 microns thick, at rotation rates of from .015 to 2.0 mega-revolutions/sec. yield values of α from 9 to 0.3 and reveal a strong increase in the damping at low frequencies. This damping is one to two orders of magnitude larger than that determined from ferromagnetic resonance line widths, and larger than can be accounted for by the original Landau-Lifshitz equation. Some of the possible origins of this large damping, and the phenomenological significance of the frequency dependence are briefly discussed.

1. INTRODUCTION

One of the presently outstanding problems of ferromagnetism is that of clarifying the nature and origin of anomalous damping, i.e., that part of the damping which cannot be attributed to eddy currents alone. The problem is a complex one because there is reason to believe that many different mechanisms contribute to the damping. Of these, only two have been clearly identified so far. One is the damping caused by exchange stiffness and eddy currents, which has been clarified by Rado^{1,2}. The other is the relaxation of the anisotropy torque associated with the presence of ferric ions in ferrites, which has been identified by Galt³. In regard to other mechanisms, the situation is

¹G. T. Rado and J. R. Weertman, Phys. Rev. 94, 1386 (1954).

²W. S. Ament and G. T. Rado, Phys. Rev. 97, 1558 (1955).

³J. K. Galt, Phys. Rev. (to be published). An oral presentation of this work was given at the Armour Symposium on Relaxation and Remagnetization in Ferromagnetic Materials in Chicago, May 26-27, 1955.

still rather chaotic. The amount of experimental data is meagre, and adequate phenomenological theories for correlating the data are lacking.

The contributions reported herein pertain to the problems of obtaining more extensive and accurate experimental data and of correlating these data by phenomenological calculations. They are, specifically:

- (1) A previously unexplored method of determining the anomalous damping by measuring the torque on a thin ferromagnetic disk in a strong rotating field.
- (2) A modification of the phenomenological damping term in the spin-wave equation which remedies certain deficiencies of the Landau-Lifshitz damping term.
- (3) A new solution of the damped spin-wave equation.
- (4) Preliminary experimental measurements of the anomalous damping in 4-79 Molybdenum Permalloy at .015, .032, 1.0 and 2.0 mega-revolutions/sec.

2. THE EXPERIMENTAL ARRANGEMENT

The experimental arrangement is shown in Figure 1. The rotating field is produced by two coils oriented at right angles in space and with exciting currents 90° out of phase. The coils produce a rotating magnetic field in the plane of the disk. This field must be strong enough to saturate the disk in order to obtain interpretable results. It is therefore necessary that the diameter/thickness ratio of the disk be large enough to keep the transverse demagnetizing field below the experimentally obtainable values of the rotating field. It is also important to keep the disk thin enough to prevent the eddy current contribution from swamping out the anomalous contribution to the torque. The latter restriction is not, however, as stringent as that imposed by the demagnetizing field.

The ferromagnetic disk is placed in a container consisting of two thin ceramic disks. This arrangement allows measurements to be made without disturbing the sample after annealing. The container and disk are supported by a conventional torsion balance arrangement. Using a 12 micron fiber, about 4 cm long, a torque constant of about .0004 dyne cm/degree is obtained, which is entirely adequate for making measurements down to about 10 Kc/sec. on a 1.3 cm disk of 4-79 Molybdenum Permalloy, 3.3 microns thick. Much greater sensitivity could be obtained by using a smaller fiber, since the torque constant is proportional to the fourth power of the radius. The only limitation is that imposed by the weight of the container and disk.

As the magnetic field rotates, the magnetization in the disk will rotate also. The damping and exchange forces will cause the magnetization to lag the field by an angle $\phi(z)$ as shown in Figure 2. A torque, T , will be exerted on the disk. It is related to the lag angle by

$$T = \int \underline{k} \cdot \underline{M} \times \underline{H}_e d\underline{r} = M H_e V d^{-1} \int_{-d/2}^{d/2} \sin \phi(z) dz, \quad (1)$$

where M , H_e , V and d are the saturation magnetization, external field magnitude, disk volume and thickness, respectively. An explicit expression can be calculated for the lag angle in terms of the saturation magnetization, conductivity, anisotropy constant, disk dimensions, external field and a phenomenological damping parameter, α , which is taken as a measure of the anomalous damping. Using Eq. (1) and the solution for the lag angle, a relation is obtained between the anomalous damping, the torque, and other measurable quantities. This relation does not include the external field as long as

$$(K/MH_e)^2 \ll 1,$$

where K is the anisotropy constant. One can therefore calculate a fairly accurate value of the anomalous damping from the measured torque values.

3. THE EQUATIONS OF MOTION

It is customary to describe the time evolution of the magnetization field by the Landau-Lifshitz equation,⁴

$$d\underline{M}/dt = \gamma \underline{M} \times \underline{H} - (\lambda/M^2) \underline{M} \times \underline{M} \times \underline{H} \quad (2)$$

where $\underline{M}(\underline{r})$ is the magnetization field, (the magnetic moment/unit volume at each point), γ is the gyromagnetic ratio, \underline{H} is the effective field, (including the molecular field as well as the magnetic field), and λ is a phenomenological damping parameter.

Eq. (1) can be transformed to

$$d\underline{M}/dt = \gamma' \underline{M} \times [\underline{H} - (\alpha'/\gamma M) d\underline{M}/dt], \quad (3)$$

where

$$\gamma' = \gamma(1 + \lambda^2/\gamma^2 M^2)$$

and

$$\alpha' = (\lambda/\gamma M)(1 + \lambda^2/\gamma^2 M^2)^{-1} \leq 1/2.$$

Eq. (3) is obtained by substituting

$$\underline{M} \times \underline{H} = \gamma^{-1} [d\underline{M}/dt + (\lambda/M^2) \underline{M} \times \underline{M} \times \underline{H}]$$

into the damping term and using the vector identities. Eq. (3) is, however, unsatisfactory for the following reason. The anomalous torque will be found to be proportional to α' , and the value of α' one calculates from experimental measurements at low frequencies is in excess of 1/2. This is inconsistent with Eq. (2), which requires that α' be a bounded function of λ . We therefore propose to use the following damped spin-wave equation:

$$d\underline{M}/dt = \gamma \underline{M} \times [\underline{H} - (\alpha/\gamma M) d\underline{M}/dt], \quad (4)$$

where γ is the gyromagnetic ratio and α is an

independent unbounded damping constant. Eq. (4) is equivalent to Eq. (2) up to terms of the order of α^2 if we set $\alpha = \lambda/\gamma M$. Eqs. (2) and (4) are therefore interchangeable for the purpose of interpreting ferromagnetic resonance experiments, since for all reported line width measurements, the inequality $\alpha \leq 0.1$ holds.

Eq. (4) can also be written in the form

$$\underline{H} - (\alpha/\gamma M) d\underline{M}/dt + (\underline{M} \times d\underline{M}/dt)/\gamma M^2 = (\underline{M} \cdot \underline{H}/M^2) \underline{M}. \quad (5)$$

Both Eqs. (4) and (5) yield the result

$$\underline{M} \cdot d\underline{M}/dt = 0 \quad (6)$$

Any three of the set of ten equations provided by Eqs. (4), (5), and (6) are linearly independent and may be used for calculating the components of $\underline{M}(\underline{r})$. The most convenient choice for subsequent calculations are Eq. (6) and the z -components of Eqs. (4) and (5).

The effective field for the case of a single preferred axis coinciding with the x -axis is:

$$\underline{H} = \underline{H} + (2A/M^2) \underline{M} + (2K/M^2) \underline{M} \times \underline{M} \times \underline{H}, \quad (7)$$

where \underline{H} is the magnetic field, A is the exchange stiffness constant, and K is the anisotropy constant. The last two terms are the molecular fields associated with the exchange and anisotropy energies, respectively.

The three chosen equations constitute a set of non-linear partial differential equations for $\underline{M}(\underline{r})$. The boundary conditions are²

$$\underline{n} \cdot \nabla \underline{M}_x = \underline{n} \cdot \nabla \underline{M}_y = \underline{n} \cdot \nabla \underline{M}_z = 0 \quad (8)$$

where \underline{n} is a vector normal to the surface of the ferromagnet.

Maxwell's equations must be used to calculate the magnetic field, $\underline{H}(\underline{r})$. Neglecting the displacement current and using Ohm's law, they can be put in the form

$$\nabla^2 (\underline{H} - \underline{H}_d) = (\underline{H} \cdot \nabla / c^2) (d\underline{H}/dt + \underline{H} \cdot d\underline{M}/dt) \quad (9)$$

where σ is the specific conductivity in Gaussian units and where \underline{H}_d is the demagnetizing field. The boundary conditions specific for the geometry of Fig. 2 are

$$\underline{H} = \underline{H}_e \equiv H_e (\underline{i} \cos \omega t + \underline{j} \sin \omega t), \quad |\underline{z}| \geq d/2 \quad (10)$$

where H_e is the magnitude of an external field rotating about the z -axis with an angular frequency ω .

4. THE STEADY STATE SOLUTION FOR AN ISOTROPIC SHEET

4.1 The Exact Equations of Motion

We consider first the case of an isotropic sheet ($K = 0$). For this case it is possible to demonstrate the existence of a simple harmonic steady-state solution of the form:

$$\underline{M}(\underline{z}, t) = M \left\{ \underline{i} \sin \theta(z) \cos[\omega t - \phi(z)] + \underline{j} \sin \theta(z) \sin[\omega t - \phi(z)] + \underline{k} \cos \theta(z) \right\} \quad (11)$$

This form corresponds to a field of uniform magnitude rotating about the z -axis at an angle

⁴L. Landau and E. Lifshitz, Physik Z. Sowjetunion 8, 153 (1935)

$\theta(z)$ with an angular velocity ω and lagging the external magnetic field by an angle $\phi(z)$. It automatically satisfies Eq. (6), leaving two independent equations plus Maxwell's equations to be solved for θ , ϕ and H .

The existence of a solution of this form for an isotropic sheet is fairly evident from a physical viewpoint. From a purely mathematical viewpoint it is rather remarkable in view of the non-linear character of the equations of motion. The fact that it does exist can be established by demonstrating that the equations for $\theta(z)$ and $\phi(z)$ are time independent and possess a solution. The time independence of the equations for θ and ϕ will be demonstrated shortly. The existence of a solution of these equations when ω and d are not too large and H_0 is not too small will be made plausible by obtaining an explicit approximate solution.

As a consequence of the linear character of Maxwell's equations, the magnetic field will have the form,

$$H = \frac{1}{2} H(z) \cos[\omega t - \psi(z)] + \frac{1}{2} H(z) \sin[\omega t - \psi(z)] - \frac{1}{2} 4\pi M \cos\theta(z) \quad (12)$$

if M has the form given by Eq. (11). The z -component of Eq. (12) is the demagnetizing field.

The substitution of Eqs. (10), (11) and (12) into the z -components of Eqs. (4) and (5) yields, respectively

$$0 = h \sin\theta \sin(\phi - \psi) - a \frac{d}{dq} (\sin^2\theta \frac{d\phi}{dq}) - b \sin^2\theta \quad (13)$$

$$\frac{d^2\theta}{dq^2} = \sin\theta \left\{ \gamma - \cos\theta \left[1 - \frac{d\phi}{dq} \right] + h \csc\theta \cos(\phi - \psi) \right\} \quad (14)$$

where

$$h = H(z)/4\pi M \quad a = 2A/\pi M^2 d^2 \quad q = 2z/d$$

$$b = \omega a / 4\pi \gamma M \quad \gamma = \omega / 4\pi \gamma M \quad h_0 = H_0 / 4\pi M \quad (15)$$

Eqs. (13) and (14) do not contain t ; hence, the assumption that M has the form given by Eq. (11) is justified, provided that Eqs. (13) and (14) are solvable.

The successive terms in Eq. (13) correspond to the torque exerted on the magnetization by the magnetic field, the exchange forces, and the anomalous damping forces, respectively. If one integrates over the thickness to obtain the total torque, the exchange contribution vanishes. If the total torque,

$$T = M^2 V h_0 d^{-1} \int_{-d/2}^{d/2} \sin\theta \sin\phi dz,$$

exerted by the external field on the magnetization is separated out, one obtains the anticipated result that this torque is equal to the torque transmitted to the lattice by eddy current and anomalous damping forces, and that the torque vanishes when there is no damping.

When the sheet is not (on the average), isotropic, an additional time-dependent term corresponding to the torque exerted on the magnetization by the anisotropy field of the lattice will appear in Eq. (13). Eq. (11) is then invalid, a not unexpected result. We consider this case in more detail in Section 4.3.

Using Eqs. (11) and (12), Maxwell's equations (Eq. (9)) reduce to

$$d^2(h \cos\psi)/dq^2 = \gamma(\sin\theta \sin\phi + h \sin\psi) \quad (16)$$

$$d^2(h \sin\psi)/dq^2 = -\gamma(\sin\theta \cos\phi + h \cos\psi) \quad (17)$$

where

$$\gamma = \pi \omega d^2 / 10^9 \rho \quad (18)$$

if ρ is in ohm-cm. Eqs. (13), (14), (16), and (17) are exact for an infinite, isotropic sheet.

4.2 Calculation of the Lag Angle

An explicit solution of the steady-state equations is needed only for calculating the torque on disks of the order of 0.1 to 10 microns in thickness for fields from 1 to 100 oersteds in magnitude at rotation rates up to 10⁷ rps. Using these limiting values, assuming $A \approx 2 \times 10^{-6}$ erg/cm and using the values $M = 600$ e.m.u., and $\rho = 6 \times 10^{-5}$ ohm cm, which correspond to 4-79 Molybdenum Permalloy, the following approximate limiting values for the constants defined in Eqs. (15) and (18) are obtained

$$10^{-4} \leq h_0 \leq 10^{-2} \quad 3 \cdot 10^{-6} \leq a \leq 3 \cdot 10^{-2}$$

$$\gamma \leq 4 \cdot 10^{-4} \quad \gamma \leq 3 \cdot 10^{-3} \quad (19)$$

We shall introduce approximations consistent with these values. In addition, we shall assume that $\phi^2 \ll 1$ and introduce approximations consistent therewith. It can be verified that this last approximation is valid as long as

$$h_0^2 \gg (b + \gamma/3)^2,$$

and will therefore always obtain if a sufficiently strong field is used.

Introducing the appropriate approximations, Eq. (14) reduces to

$$\frac{d^2\theta}{dq^2} = \sin\theta(\gamma - \cos\theta) \quad (20)$$

The only solution consistent with the boundary conditions is

$$\cos\theta = \gamma \quad (21)$$

This result justifies the use of the approximation

$$\sin\theta = 1 \quad (22)$$

in all subsequent calculations.

The solution of Maxwell's equation for the eddy current field in terms of the magnetization field is a straightforward procedure. Making the appropriate approximations, and noting that

$$\psi \leq \phi, \text{ so } \sin\psi \approx \psi, \text{ and } \cos\psi \approx 1,$$

we obtain:

$$h = h_0 \quad \psi = (\gamma/2h_0)(1-q^2) \quad (23)$$

This approximate solution is valid as long as

$$h_0^2 \gg (\gamma/2)^2.$$

Using Eqs. (22) and (23) and the approximations $\sin\phi \approx \phi$, and $\cos\phi \approx 1$, Eq. (13) reduces to

$$d^2\phi/dq^2 - k^2\phi = -a^{-1}[\eta(1 - q^2)/2 + b] \quad (24)$$

where $k^2 = h_e/a$. The solution for the boundary conditions (viz. $d\phi/dq = 0$ at $q = \pm 1$) is

$$\phi(q) = \frac{b + \eta(1 - q^2)/2}{h_e} + \frac{\eta}{2h_e} \left[\frac{2\cosh(kq)}{k \sinh(k)} - \frac{2}{k^2} \right] \quad (25)$$

When the exchange stiffness is very small

($A \rightarrow 0$, $k \rightarrow \infty$), Eq. (23) reduces to

$$\phi_0(q) = b/h_e + \psi(q) \quad (26)$$

where $\psi(q)$, the lag angle of the magnetic field, is obtained from Eq. (23). When the exchange stiffness is very large, ($A \rightarrow \infty$, $k \rightarrow 0$), Eq. (25) reduces to

$$\phi_\infty(q) = (b + \eta/3)h_e \quad (27)$$

When the exchange stiffness is finite, the solution has the form shown in Figure 3.

It is to be noted that if one passes to the limit $A \rightarrow \infty$, $k \rightarrow 0$ in Eq. (24), the result

$$d^2\phi/dq^2 = 0$$

is obtained, which tells us only that ϕ must be a constant. To obtain Eq. (27) by this direct procedure it is necessary to integrate Eq. (24) over the tape thickness before passing to the limit. This integration yields the exchange-independent relation

$$\bar{\phi} = (b + \eta/3) h_e \quad (28)$$

where $\bar{\phi} = (1/2) \int_{-1}^{+1} \phi(q) dq$.

If one now passes to the limit, the result $\phi(q) \rightarrow \bar{\phi}$ is obtained, so Eq. (27) follows. This direct approach will be useful for estimating anisotropy effects.

The dispersion in the lag angle is

$$\Delta\phi = \phi(0) - \phi(1) = \frac{\eta}{2h_e} \left(1 + \frac{2}{k \sinh(k)} - \frac{2}{k \tanh(k)} \right) \quad (29)$$

This angular dispersion could, in principle, be determined from measurements of the dependence of the mean amplitude of the magnetization (which is proportional to $\cos\Delta\phi \approx 1 - \Delta\phi^2/2$) upon the external field amplitude. In practice, this small amplitude variation is entirely masked by extraneous effects due to transverse demagnetizing fields and the tendency for the formation of an unsaturated configuration when the magnitude of the field is decreased.

The thickness dependence of the angular dispersion implies certain consequences which are of some interest. It may be seen from Fig. 3 that the angular dispersion in a 3 micron

sheet of 4-79 Molybdenum Permalloy for a rotation rate of 10^6 rps should be of the order of 1 degree. If this result is extrapolated to a 25 micron (1 mil) sheet, (momentarily ignoring the fact that the solution breaks down for large lag angles), an angular dispersion of the order of 60° is obtained. This leads one to expect that if the magnetization field were to retain its simple z dependent form as the sheet thickness was increased to 25 or 50 microns, a structure of the following form would eventually obtain: an inner region magnetized in one direction with two surface regions magnetized in an almost opposite direction and separated from the inner region by domain walls parallel to the surface. The formation of the walls would be due to a balance between the eddy current and exchange fields rather than between the anisotropy and exchange fields as is the case for ordinary static walls. Such pseudowalls cannot occur in steady-state experiments because the form of the steady state solution given by Equation (11) cannot be maintained, even in principle, for $\phi(0) > 90^\circ$, and, in practice, it appears to break down for much smaller values. Such walls could, however, form temporarily under transient conditions — when, for example, the external field was abruptly rotated by 180° . Experiments on the remagnetization of thin Molybdenum Permalloy tapes by pulse excitation give some evidence that these dynamic walls do occur in tapes thicker than about 25 microns, but not in tapes of the order of 3 microns in thickness^{5,6}.

4.3 Calculation of the Torque for an Isotropic Sheet

The relation between the average torque on the disk and the damping constants follows immediately from Eqs. (1), (15), (18), (25), and the approximation $\sin\phi \approx \phi$.

$$T = \mu_0 M^2 V (b + \eta/3) = M^2 V \omega (\alpha/\gamma M + \mu_0^2 d^2/3 \cdot 10^9 \rho) \quad (30)$$

This torque may be written as

$$T = T_a + T_e$$

where

$$T_a = M V \omega \alpha / \gamma \quad (31)$$

is the anomalous torque and

$$T_e = (2B_0^2 d^2 V / 3 \cdot 10^9 \rho) (\omega / 2\pi) \quad (32)$$

is the eddy current torque. Here T is the total measured torque, $M = B_s/\mu_0$ is the saturation magnetization, V is the disk volume, $\omega/2\pi$ is the rate of rotation of the field in revolutions/sec., d is the disk thickness, ρ is the resistivity in ohm-cm and α is the anomalous damping constant. (The relation $\alpha = \lambda/\gamma M$, where λ is the Landau-Lifshitz constant, holds if $\alpha^2 \ll 1$). It is to be noted that the torque is independent of the external field. This result has three important consequences:

5. H. Ekstein, and J. M. Kelly, Phys. Rev. 94, 1440 (1954)

6. T. L. Gilbert, J. M. Kelly and H. Ekstein, Phys. Rev. 98, 1200 (1955)

(1) It makes possible a sensitive check as to whether the disk is saturated. Below saturation the torque will be field dependent because both the average magnetization and the mean damping will be field dependent. Above saturation the torque becomes constant. This check for saturation is much more precise and reliable than measurements of the field dependence of the average magnetization by means of a search coil.

(2) It makes possible the elimination of errors due to the coercive force, random local fields (the anisotropy fields of randomly oriented grains, etc.) and a non-vanishing average anisotropy. The contributions to the torque from any of these phenomena will decrease as the field is increased; hence they can be minimized by working at large fields. (This will be proved explicitly for the anisotropy contribution). The field independence of the torque will be a means of checking the contribution from such effects.

(3) It results in a unique relation between the anomalous damping and the disk geometry, saturation magnetization, rate of rotation, resistivity, and torque. All of these quantities can readily be determined with considerable accuracy, so the anomalous damping can be determined with considerable accuracy.

The torque is also independent of the exchange stiffness. This is to be expected insofar as the exchange stiffness does not perturb the eddy current distribution because the exchange torque is entirely an interaction of one spin on its neighbors. There will be an exchange-stiffness dependent correction to the torque which is due to a perturbation of the eddy current distribution when $\Delta\phi$ becomes large. We shall not attempt to calculate this correction because it will be unimportant at the field strengths used for the rotational damping experiments.

5. THE STEADY STATE SOLUTION AND TORQUE CORRECTIONS FOR AN ANISOTROPIC SHEET

When the disk is not isotropic, there will be an additional contribution to the torque. In first approximation, at high fields, this added contribution will consist solely of an alternating torque component which is not observed in a measurement of the average torque. In second approximation, the anisotropy will perturb the motion of the magnetization so it no longer rotates at a uniform rate. The rate of rotation will be a little greater as the magnetization approaches a preferred axis, a little less as it leaves. This perturbation of the motion, which will decrease as the field magnitude increases, will increase the constant component of the torque. The magnitude of this contribution can readily be calculated for a sheet with a single preferred axis parallel to the surface.

The result $\sin\theta \approx 1$ is not altered by the introduction of anisotropy effects provided the anisotropy constant is not unduly large. The torque equation (Eq. (13)), must however, be altered by the inclusion of the anisotropy torque. This is done by substituting Eq. (7) into Eq.

(4), without dropping the anisotropy term, and using the z-component as before. Eq. (11) is no longer valid as it stands because the torque equation is no longer time-independent. However, it can be used if we allow ϕ to be time dependent. The torque equation then becomes:

$$0 = h \sin(\phi - \psi) - a \frac{\partial^2 \phi}{\partial q^2} - b(1 - \dot{\phi}/\omega) - C \sin(2\omega t - 2\phi) \quad (33)$$

where $C = K/4\pi M^2$. The eddy current equations can be calculated in essentially the same manner as before, with only the minor modifications introduced because ψ is now time dependent. We obtain in place of Eq. (23):

$$h = h_e, \quad \psi = (\gamma/2h_e)(1 - q^2)(1 - \dot{\phi}/\omega) \quad (34)$$

The assumption that $\phi^2 \ll 1$ and $\psi^2 \ll 1$ at all times has been made in deriving this result. This condition is satisfied as long as

$$(C/h_e)^2 = (K/4\pi M h_e)^2 \ll 1.$$

The equation for ϕ follows from Eqs. (33) and (34)

$$\begin{aligned} \partial^2 \phi / \partial q^2 - k^2 \phi &= \\ &= -a^{-1} \left[\gamma(1 - q^2)/2 + b \right] (1 - \dot{\phi}/\omega) \\ &\quad - a^{-1} C \sin(2\omega t - 2\phi). \end{aligned} \quad (35)$$

Exchange effects give an entirely negligible torque contribution in an isotropic sheet, so we can assume that they will also give only negligible higher order contributions to the torque in an anisotropic sheet. It is therefore permissible to consider only the solution for the limiting case $A \rightarrow \infty$, $K \rightarrow 0$. Proceeding in the same manner as for Eq. (28), one obtains the following first order non-linear equation for ϕ :

$$\phi = \bar{\phi}(1 - \dot{\phi}/\omega) + (C/h_e) \sin(2\omega t - 2\phi), \quad (36)$$

where $\bar{\phi}$ is the constant which is now defined by Eq. (26).

To calculate the correction to the constant component of the torque, the solution is expanded in powers of $\bar{\phi}$.

$$\phi = f(t) + \bar{\phi}g(t) + \dots \quad (37)$$

The equations for f and g are readily found to be

$$\begin{aligned} f(t) &= + (C/h_e) \sin[2\omega t - 2f(t)] \\ g(t) &= 1 - \dot{f}/\omega - 2(C/h_e)g \cos[2\omega t - 2f(t)] \\ &= \left\{ 1 + 2(C/h_e) \cos[2\omega t - 2f(t)] \right\}^{-2} \end{aligned} \quad (39)$$

The function $f(t)$ is an odd periodic function of t which can give no contribution to the constant component of the torque. Up to terms of the order of $(C/h_e)^3$ it is,

$$f(t) = (C/h_e) \sin 2\omega t - (C/h_e)^2 \sin 4\omega t. \quad (40)$$

The function $g(t)$ does have a constant component. Expanding Eq. (39) and substituting the result for f yields, up to terms of order $(C/h_e)^3$,

$$\begin{aligned}
g(t) &= 1 - 4(C/h_0)\cos(2\omega t - 2f) \\
&+ 12(C/h_0)^2\cos^2(2\omega t - 2f) \\
&= 1 - 4(C/h_0)\cos 2\omega t \\
&+ 10(C/h_0)^2\cos 4\omega t + 2(C/h_0)^2 \quad (41)
\end{aligned}$$

Keeping terms up to order $(C/h_0)^2$ and $(C/h_0)^3$ in the constant and periodic components, respectively, Eqs. (37), (40) and (41) yield

$$\phi = (C/h_0)\sin 2\omega t + \bar{\phi} [1 + 2(C/h_0)^2] \quad (42)$$

The instantaneous torque with anisotropy is, using Eq. (1)*,

$$T_t = T \left[1 + \frac{7}{4} (K/MH_0)^2 \right] + KV\sin 2\omega t \quad (43)$$

where T is the isotropic torque given by Eq. (30). The periodic term in Eq. (43) can easily be larger than the constant term; however, this will not affect the measurements because the torque meter effectively filters out the periodic torque components. The only important restriction is that the inequality $(K/MH_0)^2 \ll 1$ should hold so the higher order correction terms in the constant component of the torque can be ignored. When the strong inequality is satisfied, anisotropy effects can be entirely ignored, except for very precise work. The inequality is but rarely a severe restriction. When working with polycrystalline sheets, a value of K corresponding to the average anisotropy should be used, which is much less than the intrinsic anisotropy. In this case the inequality will usually be satisfied if the disk can be saturated. For nickel-iron alloys of most compositions the inequality will usually be satisfied even for a single crystal sheet.

5. PRELIMINARY EXPERIMENTAL RESULTS

The results of preliminary measurements of the torque as a function of the field amplitude on disks cut from commercially-rolled 4-79 Molybdenum Permalloy are presented in Fig. 4

The disks were annealed in dry hydrogen at 1000°C for 2 hours and allowed to cool outside the furnace, but still in a hydrogen atmosphere. Measurements of the torque as a function of the external field amplitude were made at .015, .032, 1.0 and 2.0 mega-revolutions/sec. The current source at the two lowest frequencies was a conventional high fidelity audio amplifier driven by a Hewlett Packard Model 656A Test Oscillator. This arrangement gave field amplitudes up to 16 oersteds. The current source at one megacycle was a cathode follower consisting of ten 6CD6 tubes in parallel, also driven by the Hewlett Packard

*The approximation $\sin(C/h_0) \approx C/h_0$ has been used. Substituting Eq. (40) into Eq. (3) without making this approximation yields:

$$\begin{aligned}
T_t &= T \left[1 + 2(K/MH_0)^2 \right] J_0(K/MH_0) + T^* \left[1 + 2(K/MH_0)^2 \right] \\
&\sum_{n=1}^{\infty} J_{2n}(K/MH_0) \cos 2n\omega t - MH_0 V \sin \left[(K/MH_0) \sin 2\omega t \right]
\end{aligned}$$

where $J_n(x)$ are Bessel functions.

Test Oscillator. A maximum of around 7 oersteds could be obtained with this arrangement at one megacycle. The current source for measurements at two megacycles was a push-pull tuned plate tuned grid oscillator using two 304TL tubes. It was capable of producing a field of well over a hundred oersteds - more than enough to melt the solder joints at full output.

The flattening out of the torque - field curves for high fields, in accordance with predictions, is very evident at 2.0 megacycles. At one megacycle the available power was inadequate to do more than barely reach saturation. Although it is not completely certain that saturation was actually obtained at one megacycle, we have assumed, for the purpose of calculating the damping parameter, that the disk is saturated at the highest field attained, viz., 6.7 oersteds. The bases for this assumption are: (1), the fact that the disk saturates with 6 oersteds at 2 megacycles and (2), the assertion that the threshold saturation field should not decrease as the frequency increases. Although it has not yet been established beyond all reasonable doubt that the disks were completely saturated for the highest fields used at the other rotation rates, the plateau is sufficiently pronounced to justify the assumption that saturation is practically complete.

There are two rather puzzling features of the torque-field curves below saturation. One is the large and apparently frequency-independent difference between the static and dynamic threshold saturation fields (i.e., the fields necessary to just saturate the disks under static and under dynamic conditions, respectively). The other is the maximum in the torque-field curve and its disappearance at high rotation rates.

The criterion for saturation of the disk under dynamic conditions is the flattening out of the torque-field curve. This appears to occur at about 6 oersteds for all cases where saturation was actually observed. The static threshold field was not actually measured; however, it can be estimated as follows. The demagnetizing field, calculated on the assumption that the disk is a prolate spheroid, is approximately 2 oersteds. The hysteresis loop, which was measured on a ten wrap core of the same material, is fairly rectangular and appears, for all practical purposes, to reach saturation at fields well under one oersted. The coercive force is under 0.1 oersted. The static saturation field should not, therefore, exceed three oersteds, which is only one-half of the dynamic saturating field at both .015 and 2.0 mega-revolution/sec.

A possible explanation of the difference between the static and dynamic threshold fields may be based on the presumption that even when the disk is apparently saturated under static conditions, there are still a few reverse domains (or areas of reverse magnetization if a discrete domain structure is lacking). When the magnetization rotates, the motion of these regions will be strongly damped, because the rate of rotation of the spins in the regions which are not uniformly magnetized will be higher than elsewhere. When this damping is strong enough to prevent the reverse domain

structures from being dragged around with the rest of the magnetization, surrounding regions of the magnetization may also be held back because of dipole-dipole interaction. The originally small deviation from saturation under static conditions can thus become quite pronounced under dynamic conditions. If this added deviation does occur, it will only disappear at field magnitudes for which the torque exerted on the unsaturated region is strong enough to make the entire static structure rotate. This magnitude can be expected to be somewhat higher than the static threshold field.

The weakness of this explanation is its inability to account for the apparent frequency independence of the difference between the static and dynamic threshold saturation fields. One would expect the difference to increase with frequency if the above explanation were valid. Further study and more data are needed to clarify this matter.

The maximum in the torque curve can possibly be explained as follows. As the external field decreases from above saturation to zero, there are two contending effects. One is the increase in the damping because of the higher local rate of rotation in the walls of the reverse domains. This tends to increase the torque. The other is the decrease in the average magnetization, which tends to decrease the torque. If the first effect is dominant just below threshold saturation, the torque curve will rise to a maximum before it ultimately drops to zero as the field decreases to zero.

The disappearance of the maximum at high rotation rates is more difficult to understand. One may expect the succession of domain configurations which occur as the magnitude of the rotating field decreases to be dependent on the rate of rotation. It is conceivable that this dependence is such as to decrease the relative contribution to the torque from the increased damping in unsaturated regions until this contribution is no longer dominant just below threshold saturation. However, it is then difficult to understand how this could occur without any appreciable change in the threshold saturation field. Again, more data is needed for clarification.

Both of the puzzling features just discussed involve the detailed structure of the magnetization field below saturation. They are, therefore, of less fundamental interest than the quantities observed in the region of saturation where the domain structure is presumably simple, well-defined and field-independent.

The results of measurements in the region of saturation are presented in Fig. 5.* The most significant feature of these results is the pronounced increase in the damping parameter at the lower rotation rates..

A comparison of the rotational damping with the damping determined from the resonance line width and domain wall velocity measurements is given in Fig. 6.** The most striking result of this comparison is the order of magnitude increase of the damping parameter obtained from torque measurements over the same

phenomenological parameter obtained by the resonance and wall velocity methods.

Before discussing the significance of these experimental results, it should be emphasized that they are of a preliminary nature. We are not yet in a position to assert that the observed anomalous damping is due to intrinsic, structure-independent effects. It is unlikely that the disk was completely saturated in the strict sense that the magnetization was everywhere parallel to itself. Edge effects due to the fact the disk was a very flat cylinder rather than a true prolate spheroid, surface irregularities, residual stresses, etc would all tend to favor the formation of some regions of reverse magnetizations. It is possible that these regions could have a dynamic effect which was out of all proportion to their size. Specifically, it is conceivable that a deviation of less than 1 per cent from true saturation could cause an appreciable difference in the damping. Experiments for checking this important matter are in progress. Until they are complete, we cannot be sure whether the observed order of magnitude difference between resonance and rotational damping is a structure sensitive or an intrinsic phenomenon.

In regard to the significance of the large, frequency dependent rotational damping constant, we have only two points to make at the present time. The first point is that the damping at low frequencies exceeds the maximum value obtainable from the Landau-Lifshitz phenomenological damping term. The modified damping term introduced in Eq. (4) must, therefore, be used if one desires to express both the damping at different rotation rates and the damping observed by different methods of measurement in terms of a single local damping parameter.

The second point is that even the modified damping term cannot correctly describe all the observed damping, for the following reasons. The use of either the Landau-Lifshitz or the modified damping term carries with it the implicit assumption that the damped spin wave equation is valid for arbitrary motion of the magnetization field. This assumption is contradicted by the observed frequency dependence of α . The damping at 1 and 2 Mrps appears to be constant and may therefore be described in this phenomenological manner.

*It should be pointed out that the uncertainty in the value of the saturation magnetization, $M = 7400/\text{gauss}$, was ± 8 per cent. At low frequencies this will only produce an uncertainty of ± 8 per cent in α . At 1 and 2 Mrps, for which the eddy current correction amounts to half the total, the uncertainty in α from this source is about ± 30 per cent.

**In specifying the frequency for wall velocity measurements, the rate of rotation of the spins in the center of the wall was taken. Since the damping is calculated from the dependence of the wall velocity on the driving field, it must be assigned to a range of frequencies rather than to a single frequency. The same remarks hold for the assignment of a frequency to the remagnetization measurements.

However, the additional damping which appears at lower rotation rates cannot be correctly described by either Eq. (2) or Eq. (4).

There is no obvious modification of the original Landau-Lifshitz equation which will account for a frequency dependence of the damping parameter. In the case of the modified form given by Eq. (4) one can, however, give a consistent phenomenological description of frequency dependent damping by an obvious further modification. We replace the quantity $\alpha \underline{M}$ in the damping term by

$$\sum_{n=0}^{\infty} a_{2n+1} d^{2n+1} \underline{M} / dt^{2n+1}$$

to obtain*

$$\dot{\underline{M}} = \underline{M} \times \left[\underline{H} - \gamma^{-1} \underline{M} - \sum_{n=0}^{\infty} a_{2n+1} d^{2n+1} \underline{M} / dt^{2n+1} \right] \quad (44)$$

Insofar as the steady state solution for the isotropic case is concerned, the only effect this modification has on the final expression for the torque is to replace the constant α by the quantity

$$\alpha(\omega) = \sum_{n=0}^{\infty} a_{2n+1} \omega^{2n} \quad (45)$$

The constants a_{2n+1} may then be chosen to fit the experimental data. Eq. (44) would be miserable to solve for a general motion of the magnetization field; however, it does provide a consistent phenomenological description of the rotational damping experiments when the damping parameter is frequency dependent, without abandoning what meagre advantages may accrue from the use of local damping.

*Even derivatives give no contribution to the anomalous torque.

6. RECAPITULATION

To summarize briefly, we have presented a hitherto unexplored method of measuring the anomalous damping in ferromagnetic sheets. The method consists in measuring the torque on a small disk of ferromagnetic material suspended in a strong rotating field. The method has the merits of simplicity, of providing a known domain geometry (which makes possible an explicit and accurate calculation of the contribution from eddy current damping) and of permitting measurements over a wide range of previously inaccessible frequencies which span those frequencies of interest for most technical applications.

We have also derived the relations needed to calculate the eddy current contribution to the torque and to calculate a damping parameter (or damping function) from the remaining "anomalous" torque. This damping parameter can be compared with damping parameters calculated the resonance line width in ferromagnetic resonance experiments. In connection with this derivation, a new form of the damped spin wave equation is presented. This modified form will account for an anomalous torque of any magnitude, in contrast to the Landau-Lifshitz equation which gives an upper limit to the anomalous torque, and can readily be generalized to describe the frequency dependence of the damping.

Finally, we have presented preliminary experimental results which indicate that the anomalous rotational damping at 1.0 and 2.0 mega-revolutions/sec is an order of magnitude larger than the damping determined from resonance line widths, and that the anomalous rotational damping is frequency dependent and rises markedly at lower rotation rates (15 and 32 kilo-revolutions/sec).

In conclusion, we would like to thank Dr. H. Ekstein for his advice and helpful criticism.

Table 1

Summary of Preliminary Measurements
on a 4-79 Molybdenum Permalloy Disk,
3.5 μ Thick and 1.3cm in Diameter

$\omega/2\pi$ Rotation Frequency rps	T Total Torque dyne-cm	T _e Eddy Current Torque dyne-cm	T _a Anomalous Torque (T-T _e) dyne-cm	α Damping Parameter ($\gamma T_a/\omega MV$)
.015x10 ⁶	.012	.0004	.012	9
.032x10 ⁶	.009	.001	.008	3
1.0x10 ⁶	.055	.027	.028	0.3
2.0x10 ⁶	.110	.054	.056	0.3

Table 2

Comparison of Anomalous Damping Parameters
Obtained by Different Methods

Method	Frequency Mc/sec	Material	α ($\alpha = \lambda/\gamma M$ if $\alpha^2 \ll 1$)	Reference
Ferromagnetic Resonance	24,000	Silicon Iron	~ 0.1	1
		Magnetite	0.1	2
		Nickel	.04	1
		Supermalloy (cold roll)	.03	1
		Supermalloy (annealed)	.01	1
		Nickel Ferrite	.004	3
	9,000	Nickel	.048	4
		Supermalloy	.029	4
		Nickel Ferrite	.014	5
	Wall Velocity 4 - 40 250	Magnetite	.039	6
		Nickel Ferrite	.004	6
Rotational Damping	2.0	4-79 Mo-Perm	0.3	7
	1.0	4-79 Mo-Perm	0.3	7
	.032	4-79 Mo-Perm	3	7
	.015	4-79 Mo-Perm	9	7
Remagnetization	1 - 4	4-79 Mo-Perm	1.4	8

1. Data compiled by E. Abrahams and C. Kittel, Revs. Modern Phys. 25, 233 (1953)
2. L. R. Bickford, Jr., Phys. Rev. 78, 449 (1950)
3. C. Guillaud and M. Roux, Compt. rend. 229, 1133 (1949)
4. J. A. Young, Jr. and E. A. Uehling, Phys. Rev. 94, 544 (1954)
5. D. W. Healy, Jr., Phys. Rev. 86, 1009 (1952)
6. J. K. Galt, J. Andrus and H. G. Hopper, Revs. Modern Phys. 25, 93 (1953)
7. Present Experiments
8. T. L. Gilbert, J. M. Kelly and H. Ekstein, Phys. Rev. 98, 1200 (1955)

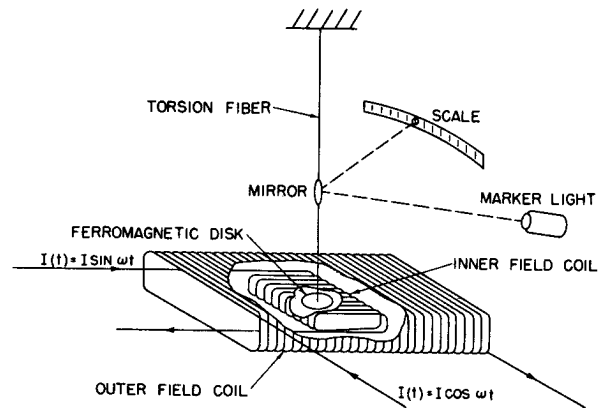


Fig. 1 Experimental Arrangement for Rotational Damping Measurements.

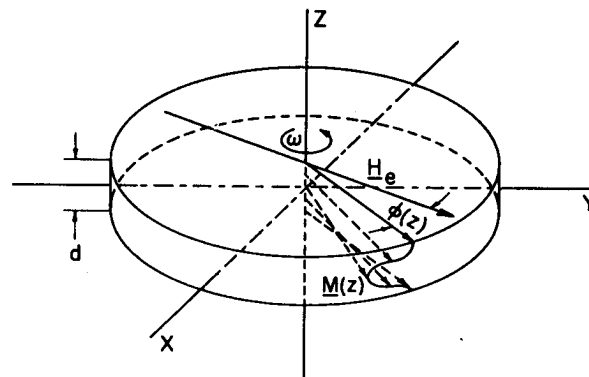


Fig. 2 Schematic representation of the magnetization field driven by a rotating external field.

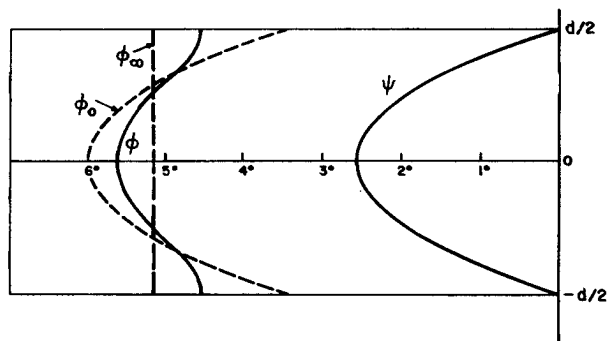


Fig. 3. The lag angle of the magnetization (ϕ) and the magnetic field (ψ) in the rotating field experiment. Calculated for $d = 3\mu$, $H_e = 3$ oe, $\omega/2\pi = 10^6$ rps, $\alpha = 0.3$, and $A = 0$, $2 \cdot 10^{-6}$ and ∞ ergs/cm.

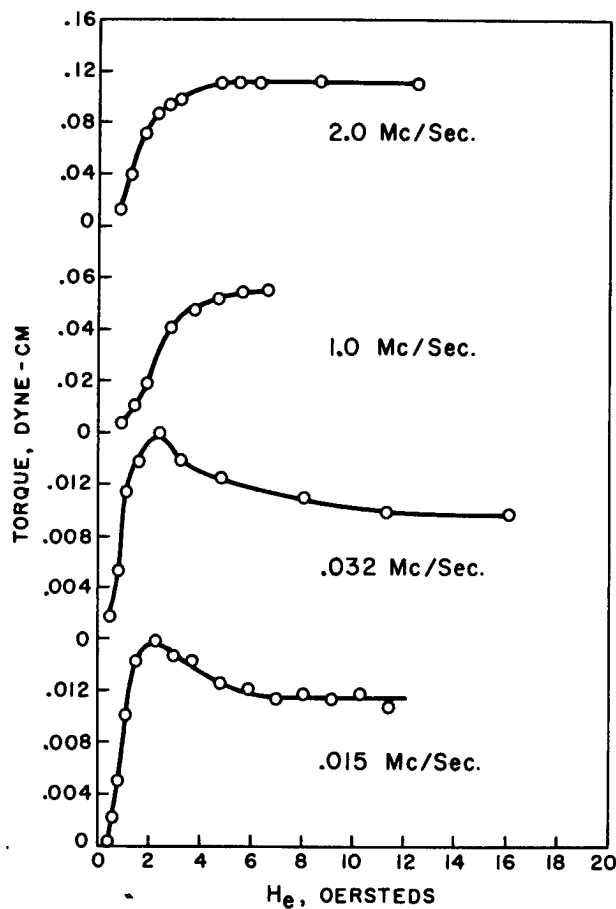


Fig. 4 Torque on a 1.3 cm disk cut from a commercially rolled 4-79 Molybdenum Permalloy sheet, 3.3 microns thick.